



## Can angiographic Flat Detector Computed Tomography blood volume measurement be used to predict final infarct size in acute ischemic stroke?

Thijs van der Zijden<sup>a,b,\*</sup>, Annelies Mondelaers<sup>a,c</sup>, Caroline Loos<sup>d,e</sup>, Maurits Voormolen<sup>a,c</sup>, Caro Franck<sup>a,c</sup>, Maarten Niekel<sup>a</sup>, Thomas Jardinet<sup>a</sup>, Thomas Van Thielen<sup>a,b</sup>, Olivier d'Archambeau<sup>a</sup>, Tomas Menovsky<sup>e,f</sup>, Paul. M. Parizel<sup>c,g,h</sup>

<sup>a</sup> Department of Radiology, Antwerp University Hospital (UZA), 2650 Edegem, Belgium

<sup>b</sup> Department of Medical Imaging, AZ KLINA, 2930 Brasschaat, Belgium

<sup>c</sup> Research Group mVision, Faculty of Medicine and Health Sciences, University of Antwerp (UA), 2610 Wilrijk, Belgium

<sup>d</sup> Department of Neurology, Antwerp University Hospital (UZA), 2650 Edegem, Belgium

<sup>e</sup> Research Group Translational Neurosciences, Faculty of Medicine and Health Sciences, University of Antwerp, (UA), 2610 Wilrijk, Belgium

<sup>f</sup> Department of Neurosurgery, Antwerp University Hospital (UZA), 2650 Edegem, Belgium

<sup>g</sup> Department of Radiology, Royal Perth Hospital and University of Western Australia Medical School, Perth, WA, Australia

<sup>h</sup> Director, Western Australia National Imaging Facility (WA NIF) Node, Perth, WA, Australia

### ARTICLE INFO

#### Keywords:

Flat detector computer tomography (FD-CT)  
Angiographic perfusion imaging  
Pooled Blood Volume (PBV) mapping  
Acute ischemic stroke  
Infarct core

### ABSTRACT

**Introduction and purpose:** Flat detector computed tomography (FD-CT) technology is becoming more widely available in the angiography suites of comprehensive stroke centers. In patients with acute ischemic stroke (AIS), who are referred for endovascular therapy (EVT), FD-CT generates cerebral pooled blood volume (PBV) maps, which might help in predicting the final infarct area. We retrospectively analyzed pre- and post-recanalization therapy quantitative PBV measurements in both the infarcted and hypoperfused brain areas of AIS patients referred for EVT.

**Materials and methods:** We included AIS patients with large vessel occlusion in the anterior circulation referred for EVT from primary stroke centers to our comprehensive stroke center. The pre- and post-recanalization FD-CT regional relative PBV (rPBV) values were measured between ipsilateral lesional and contralateral non-lesional areas based on final infarct area on post EVT follow-up cross-sectional imaging. Statistical analysis was performed to identify differences in PBV values between infarcted and non-infarcted, recanalized brain areas.

**Results:** We included 20 AIS patients. Mean age was 63 years (ranging from 36 to 86 years). The mean pre- EVT rPBV value was 0.57 ( $\pm 0.40$ ) for infarcted areas and 0.75 ( $\pm 0.43$ ) for hypoperfusion areas. The mean differences ( $\Delta$ ) between pre- and post-EVT rPBV values for infarcted and hypoperfused areas were respectively 0.69 ( $\pm 0.59$ ) and 0.69 ( $\pm 0.90$ ). We found no significant differences ( $p > 0.05$ ) between pre-EVT rPBV and  $\Delta$ rPBV values of infarct areas and hypoperfusion areas.

**Conclusion:** Angiographic PBV mapping is useful for the detection of cerebral perfusion deficits, especially in combination with the fill run images. However, we were not able to distinguish irreversibly infarcted tissue from potentially salvageable, hypoperfused brain tissue based on quantitative PBV measurement in AIS patients.

### 1. Introduction

Acute ischemic stroke (AIS) is a leading cause of disability and death in the world [1]. Today, the mainstay of primary treatment of patients with acute ischemic stroke caused by a large vessel occlusion (LVO) is endovascular mechanical thrombectomy (EVT). Well-defined clinical and imaging criteria are used for selecting patients for EVT [2]. Once a

swift and robust selection has been done, restoration of blood supply to the affected brain areas must be obtained as quickly as possible to get the best clinical outcome [3]. In clinical practice, a significant number of patients are referred from primary stroke centers to comprehensive stroke centers for EVT procedure. Due to organizational and infra-structural factors, optimal time treatment intervals are sometimes exceeded. Moreover, progression from tissue at risk to infarction can

\* Corresponding author at: Department of Radiology, Antwerp University Hospital (UZA), 2650 Edegem, Belgium.

E-mail address: [thijs.van.der.zijden@uza.be](mailto:thijs.van.der.zijden@uza.be) (T. van der Zijden).

<https://doi.org/10.1016/j.ejrad.2022.110650>

Received 24 June 2022; Received in revised form 30 October 2022; Accepted 10 December 2022

Available online 13 December 2022

0720-048X/© 2022 The Authors. Published by Elsevier B.V. This is an open access article under the CC BY-NC-ND license (<http://creativecommons.org/licenses/by-nc-nd/4.0/>).

vary considerably between individual patients [4]. This results in discrepancies in the potential clinical response to revascularization therapy among patients, despite being treated within adequate time intervals.

Conventional computer tomography (CT) and/or magnetic resonance imaging (MRI) are the cross-sectional modalities of choice for imaging in AIS patients. CT can select potential EVT candidates by using perfusion imaging and (multiphase) CT angiography. MRI can be of added value in selecting LVO acute stroke patients for EVT using diffusion and perfusion imaging [5]. The purpose is to detect the presence of potentially salvageable brain tissue (penumbra).

The introduction of flat panel technology into biplane angiographic systems has made it possible to perform flat detector CT (FD-CT) imaging in diagnostic and therapeutic procedures [6]. FD-CT provides the interventional neuroradiologist insights into parenchymal changes, vascular anatomy and perfusion, thereby obviating the need for transporting patients outside the angiography suite for cross-sectional imaging. Several studies demonstrated the valuable role of FD-CT techniques in interventional neuroradiology practice [7–11]. Current high-end biplane angiographic systems deliver perfusion imaging with quantitative dynamic perfusion parameters (e.g. cerebral blood flow (CBF), contrast transit time parameters, time to peak, etc.) [12]. Theoretically, these systems enable a full stroke work-up in the angiography suite without the need for additional conventional cross-sectional imaging modalities.

Due to limitation of C-arm rotations in short time intervals, the current standard of practice for angiographic perfusion imaging remains limited to a static parameter during a steady-state contrast injection phase, generating so-called parenchymal or pooled blood volume (PBV) maps. It is reported that FD-CT PBV values correspond with cerebral blood volume (CBV) values obtained with conventional CT [13] and MRI [14,15]. Although static perfusion imaging is more limited in use compared to dynamic perfusion imaging, the technique does have some advantages. PBV imaging only needs two imaging rotation runs (mask run and fill run), compared to multiple runs in dynamic perfusion imaging; this implies that it is less prone to motion artefacts, and decreases the radiation dose to patients. Literature data show that PBV mapping is useful to triage AIS patients by identifying potentially salvageable brain areas in the setting of acute LVO amenable for EVT [16]. In addition to PBV mapping, the mask and fill runs can be utilized for additional image analysis. The mask runs can be reformatted as non-contrast enhanced CT images to detect hemorrhage or large ischemic parenchymal changes. Assessment of vessel patency and collateral vascular status can be done by evaluating the fill runs.

To date, data on the clinical use of FD-CT PBV are still limited. Some studies suggest that PBV data are useful for evaluating potential infarct growth and collateral status prior to EVT in case of long time intervals after initial imaging [17,18], while others do not [19].

The purpose of this paper was to assess the value of FD-CT PBV measurements in AIS patients to predict the final infarct area versus the potentially salvageable hypoperfused brain area. Secondly, we also evaluated the potential of  $\Delta$ rPBV measurements between pre- and post-recanalization therapy for final infarct prediction.

## 2. Material and methods

### 2.1. Study population

From January 2016 until January 2021, 51 AIS patients undergoing angiographic FD-CT PBV mapping in a tertiary referral neuro-interventional unit were retrospectively examined. All patients were referred for EVT. Two cases of posterior circulation stroke were excluded, leaving a total of 49 patients with anterior circulation occlusion. In one patient, the intended FD-CT examination was not possible due to technical problems. From the 48 patients who underwent successful FD-CT examination, six patients were excluded because of low quality of the acquired PBV scans due to significant motion artefacts and

in one patient no correct PBV measurement could be done due to post-processing software issues.

Of the remaining 41 patients, 21 patients were further excluded from this study. They included 9 patients who showed no or very limited infarct on the follow-up cross-sectional imaging; 4 patients died without follow-up scanning; 2 patients were lost to follow-up; 6 patients only had post-recanalization FD-CT PBV scans. In patients where recanalization occurred before the intended EVT was attempted, either spontaneously or after intravenous thrombolytic therapy (IVT), the PBV datasets were classified as “post-recanalization” and were excluded for further analysis. The patient was also excluded from further analysis if no infarct on follow-up cross sectional imaging was visible, and therefore no infarct area for PBV measurement could be determined.

Finally, a total of 20 patients were included in the study, yielding 20 pre-recanalization datasets for retrospective analysis of relative PBV (rPBV) values. In 11 patients, both pre- and post-recanalization PBV imaging measurements were available. All AIS patients underwent follow-up multi-slice CT or MR examination one day post-procedure.

The study protocol was approved by the local ethics committee (Ref. nr. 21/05/062) and waived the requirement of obtaining any informed consent.

### 2.2. Clinical measurements

A retrospective search for clinical data, angiographic, procedural and post-procedural cross-sectional follow-up imaging data was performed by using the hospital’s electronic medical records and Picture Archiving and Communication System (PACS). Besides the patients demographic data, such as gender and age, the explored clinical data included times of symptom onset to groin puncture, times of groin puncture to recanalization, National Institutes of Health Stroke Scale (NIHSS) scores [20] before and after EVT, and the modified Ranking Scale (mRS) [21] at three months. The occlusion sites were registered. Procedural data included recanalization success indicated with the Thrombolysis In Cerebral Infarction (TICI) score [22], use of general or local anesthesia, used method for recanalization (EVT and/or carotid artery stenting (CAS)), number of passages and occurrence of procedural complications.

## 3. Angiographic imaging and endovascular procedure

### 3.1. Imaging protocol

Scanning was done by 3 interventional neuroradiologists: TVZ (8–13 years of experience in interventional neuroradiology), MVO (13–18 years of experience) and MNI (0–5 years of experience, under supervision of TVZ). Besides conventional angiographic work-up, implementation of angiographic PBV imaging was performed at the discretion of the interventional neuroradiologist. In general, PBV imaging was considered in case of substantial time delay between initial stroke work up imaging and time of EVT and/or in case of significantly altered clinical status at start or during EVT procedure compared to clinical status at initial imaging time. FD-CT acquisitions were performed immediately before and after EVT procedure.

Both angiographic examinations and endovascular procedures were performed on a biplane angiographic system (Artis Zee with Pure® biplane system, Siemens Healthcare GmbH, Forchheim, Germany). FD-CTP PBV imaging acquisition was done by two rotations of 6 s each, in which 397 frames were obtained in a total scan angle of 200°. The first rotation consisted of a mask run without contrast injection and the second run, the fill run, was performed after contrast injection. Contrast medium was injected through a 4 French pigtail catheter, positioned at the level of the aortic root. A total of 75 mL, consisting of a mixture of 25 mL contrast medium (Iomeron® 300, Bracco) with 50 mL saline, was injected at a rate of 5 mL/s. The fill run was carried out nine seconds after start of contrast injection. Angiographic FD-CTP PBV imaging was done during steady-state contrast quantity in the brain.

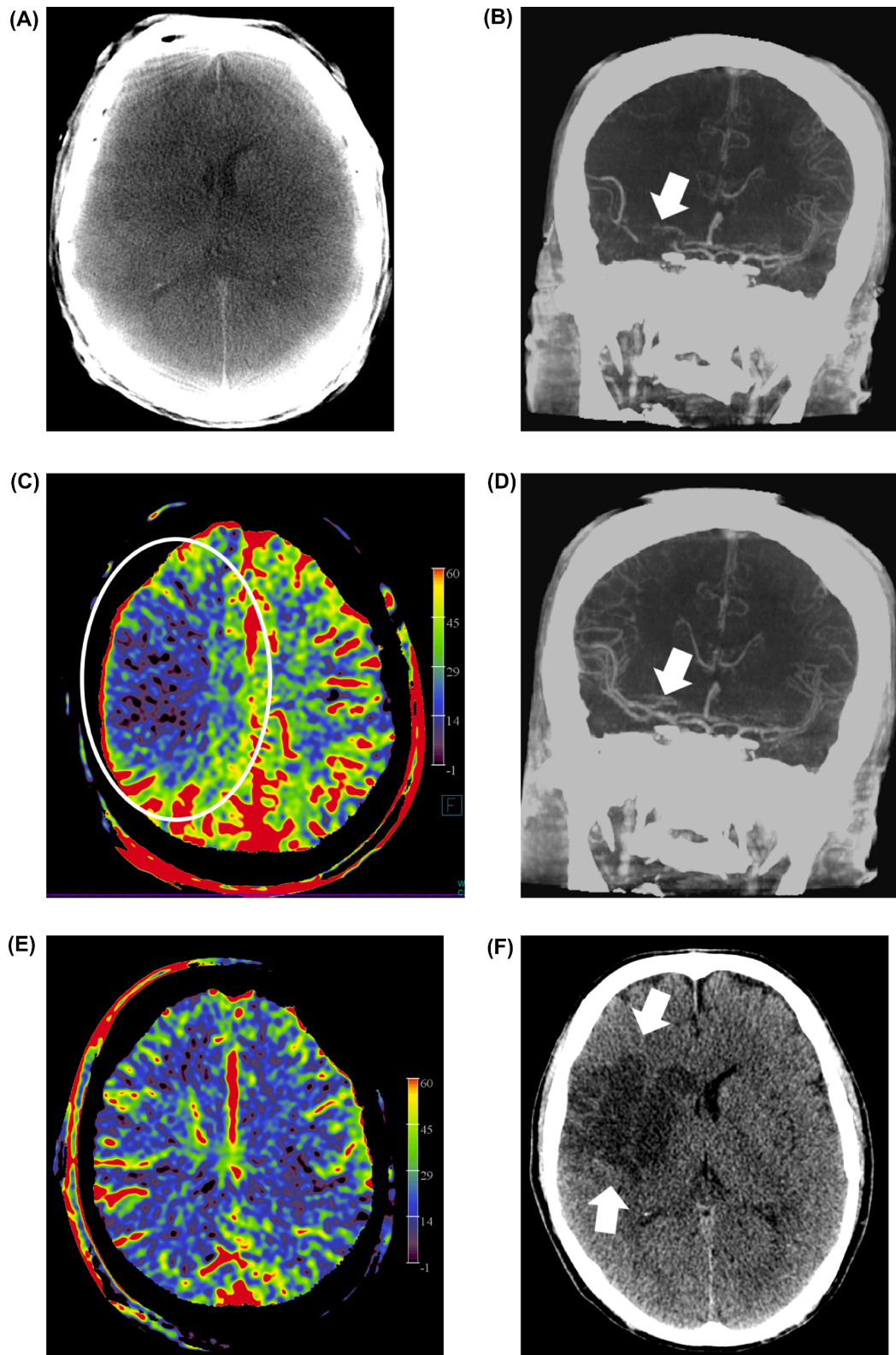


**Fig. 1.** Illustration of mask run, fill run and PBV MIP reformations in a 55-year-old patient (patient no. 13) presenting with a right carotid tip – M1 segment middle cerebral artery (MCA) occlusion. Interventional mask run MIP reformation (a) showed hypodensity at the level of the basal ganglia, however, no hemorrhage was observed. Coronal MIP reformation of the fill run pre-EVT confirmed the persistent occlusion (b, white arrow). Axial PBV MIP reformation demonstrated the low PBV area (c, white circle) at the right hemisphere, compared to the unaffected left hemisphere. Post- EVT coronal fill run MIP reformation showed recanalization (d, white arrow). Post- EVT axial PBV MIP reformation demonstrated restoration of the flow to the right hemisphere (e). One day post-EVT follow-up axial CT scan image demonstrated an infarct in the anterior MCA area (f, white arrows).



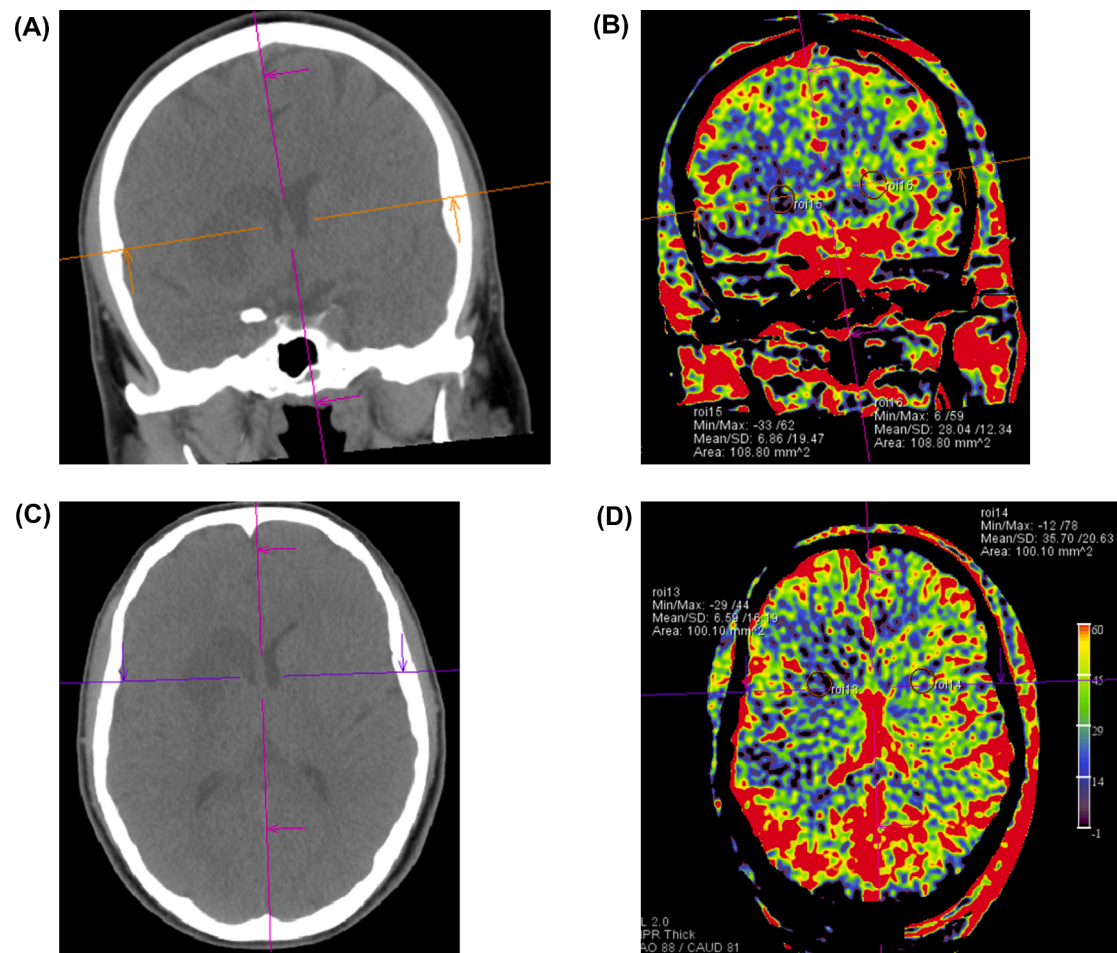


**Fig. 2.** Example of PBV value measurements for calculation of relative PBV values in a 41-year-old patient (patient no. 10) presenting with a short distal M1-segment occlusion in the right middle cerebral artery (MCA), successfully treated by endovascular recanalization. CT brain one day post-EVT showed a small infarct in the right basal ganglia (a and c). Corresponding final infarct areas on the PBV maps were localized by fusion of the PBV scans with the post-procedural CT brain scan. Intralésional PBV values on coronal (b) and axial (d) images were mirror imaged to the contralateral non-lesional area for calculation of the rPBV's.

### 3.2. Image processing

After image acquisition, colour-coded quantitative FD-CT PBV maps were calculated in units of mL contrast / 1000 mL tissue using commercially available syngo DynaPBV Neuro software (Siemens Healthcare GmbH, Forchheim, Germany). The mask runs were available for use as non-enhanced CT scan series. The fill runs were applied for rendering FD-CT angiography images. The three obtained series (mask run, fill run and PBV maps) were post-processed on a Leonardo workstation (Siemens Healthcare GmbH, Forchheim, Germany) and available for analysis in multiplanar views during the procedures. Maximum intensity projection (MIP) images in axial, sagittal and coronal views were reconstructed and stored on the PACS (Fig. 1).

We used a slice-wise relative PBV (rPBV) calculation method, adopted from Wen *et al.* (2017), which was used for tumor PBV measurements:  $rPBV = 0.5 \times (PBV_{\text{lesion axial}} + PBV_{\text{lesion coronal}}) / (PBV_{\text{healthy axial}} + PBV_{\text{healthy coronal}})$  [23]. The axial and coronal PBV values were determined by using hand drawn ellipsoidal regions of interest (ROI) surfaces in the respective planes. Reference PBV values were obtained using ellipsoidal ROI's in axial and coronal plane at corresponding contralateral brain areas. Regional PBV measurements were done in infarcted areas, in finally revascularized hypoperfused non infarction regions and not affected contralateral brain areas. For correct delineation of the final infarct regions and salvaged regions, the PBV maps were correlated with the follow-up CT or MRI images using the fusion application tool on the angiographic workstation. (Fig. 2) The difference

in rPBV values pre- and post-recanalization ( $\Delta rPBV$ ) was calculated as well, if both pre- and post-rPBV data were available (11 patients in total).

### 3.3. Endovascular procedure

Endovascular thrombectomy was done by means of stent retriever, thrombus aspiration or a combination of both. A balloon guide catheter was used in all cases. The additional radiation dose exposure associated with the added FD-CT PBV acquisitions was analyzed, using the archived dose reports of the angiographic examinations. Brain dose (BD) and effective dose (ED) of individual acquisitions were calculated using the registered dose area products with the use of a Monte-Carlo software tool (PCXMC version 2.0.1.4 Rotation, Radiation and Nuclear Safety Authority STUK, Helsinki, Finland).

### 3.4. Statistical analysis

Data analysis was performed using IBM SPSS Statistics (version 28.0, IBM Corp., Armonk, N.Y., USA). Statistical significance was defined as  $p \leq 0.05$  (two-tailed). We analyzed median rPBV and  $\Delta rPBV$  value of the infarct core and hypoperfusion areas by using the Mann-Whitney *U* test.

## 4. Results

In total, 20 patients were included in the study. Mean age at stroke

**Table 1**

An overview of the patient characteristics and radiological data.

Patient no	Age (yr)/gender	Occlusion site	General anesthesia	Procedure	Time symptom onset to groin puncture (min)	Time groin puncture to recanalization (min)	No of passages	TICI grade	NIHSS at start of procedure	NIHSS post endovascular procedure (EVT or CAS)	mRS at 3 months
1	60/F	left carotid tip and M1 MCA	yes	EVT	245	67	3	2b	21	20	2
2	69/M	left cervical ICA	no	no	330	NA	NA	NA	5	NA	3
3	69/M	left proximal M2 MCA	yes	EVT	187	25	1	2b	17	13	3
4	53/F	left M1 MCA	no	EVT	220	30	1	3	22	24	3
5	79/F	right M1 MCA	no	EVT intended, no selective catheterization possible	wake up	NA	0	0	12	NA	5
6	78/F	left carotid tip and M1 MCA	yes	EVT	222	43	2	3	17	17	2
7	67/M	left M1 MCA	no	EVT	300	57	2	2b	21	16	4
8	53/M	left cervical ICA and M1 MCA	no	EVT intended, no passage of proximal occlusion possible	227	NA	0	NA	14	14	3
9	60/M	left cervical ICA and M1 MCA	yes	EVT	232	38	1	2b	17	2	1
10	41/M	right M1 MCA	no	EVT	235	62	3	3	10	4	2
11	86/M	left carotid tip	no	EVT	220	60	3	3	20	23	6
12	67/M	left cervical ICA, no intracranial occlusion	no	CAS + thrombosuction cervical ICA	152	42	1	1	10	7	6
13	55/M	right carotid tip and M1 MCA	yes	EVT	170	23	2	2b	17	12	2
14	78/M	right carotid tip and M1 MCA	no	EVT	143	31	1	3	14	10	6
15	73/F	right M2 MCA	no	EVT	327	58	1	2b	13	0	3
16	57/M	left cervical ICA and M2 MCA	no	EVT	525	40	1	2b	12	15	2
17	49/M	right M1 MCA	no	EVT	280	59	3	1	8	3	0
18	36/M	left cervical ICA	no	CAS	300	NA	0	NA	17	17	4
19	64/M	right M1 MCA	no	EVT	210	26	1	2b	13	10	3
20	72/M	right M1 MCA	no	EVT	150	30	1	3	12	5	0

CAS indicates cervical Carotid Artery Stenting; EVT, endovascular therapy; ICA, internal carotid artery; F, Female; M, male; MCA, middle cerebral artery; mRS, modified Ranking Scale; NA, Not Applicable (no EVT performed); TICI, Thrombolysis In Cerebral Infarction; NIHSS, National Institutes of Health Stroke Scale.

presentation was 63 years ranging from 36 to 86 years. Fifteen (75 %) of included patients were male. In one case, the time of onset of clinical symptoms was not known (i.e. wake up stroke). The median NIHSS at presentation was 14, ranging from 5 to 22.

Occlusion sites were the carotid tip in 5 patients (25 %), middle cerebral artery (MCA) M1-segment in 7 patients (35 %), and proximal MCA M2-segment in 2 patients (10 %). In 3 patients (15 %), an isolated cervical internal carotid artery (ICA) occlusion was present. Furthermore, 3 patients (15 %) had a tandem lesion. In 12 cases (60 %), the occlusion sites were on the left side, with 8 occlusion sites on the right. All the occlusions at the level of the cervical ICA were on the left side (6 patients, 30 %).

Median time of symptom onset to groin puncture in the patients with

known time of symptom onset was 227 min (range 143–525 min). General anesthesia was applied in 5 cases. Median time from groin puncture to recanalization was 41 min, ranging from 23 min to 67 min.

In one case (patient no. 2), recanalization procedure was not pursued due to low NIHSS and only cervical occlusion site at time of presentation in the angiography suite. In the other case (patient no 18), only CAS was performed without thrombectomy. In 14 of 18 patients (78 %), in which EVT was attempted, recanalization procedure was successful (TICI score 2b or 3). In one case, selective catheterization of the carotid artery was not possible due to tortuosity (patient no. 5, TICI 0). In one patient with tandem occlusion, the proximal occlusion was not passable, no EVT of the distal occlusion could be done (patient no. 8, TICI score 0). Only limited recanalization occurred in 2 cases (patient no. 12 and 17, TICI

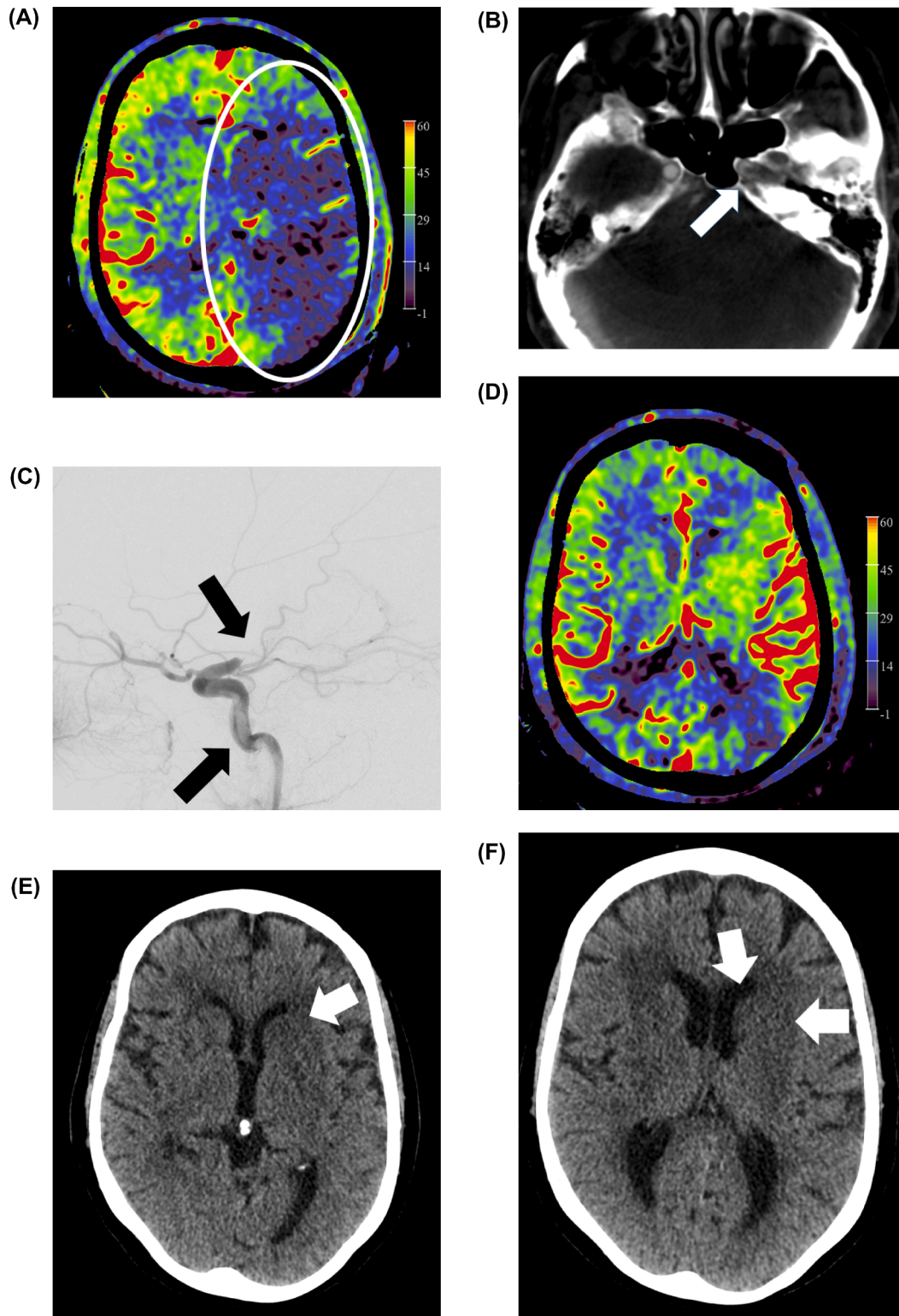


**Fig. 3.** A 78-year-old female patient presented with a left MCA stroke to a primary stroke center (patient no. 6). The clinical symptoms worsened significantly after starting IVT (NIHSS score deteriorated from 4 to 17). Therefore the patient was referred for EVT. Pre-intervention FD-CT PBV imaging showed a large volume of lowered CBV value at the left hemisphere (a, ellipsoid). MIP reformations of the pre-intervention fill run confirmed not only M1-segment occlusion of the left MCA (not shown), but demonstrated thrombus in the left proximal intracranial internal carotid artery (ICA) (b, white arrow). As a note, this finding was not reported during initial imaging at the referring center. Subsequent angiographic runs with selective left ICA injection confirmed both vascular lesions (c, black arrows). Post-recanalization FD-CT imaging demonstrated low infarct PBV values and elevated PBV values in the revascularization hypoperfusion area (d). Post-treatment CT brain follow-up the next day showed no hemorrhagic complications with infarct confined to the basal ganglia (e and f, white arrows). An interesting finding is the high mismatch in pre-EVT PBV lesion volume and final infarct volume.

**Table 2**  
Summary of rPBV values and  $\Delta$ rPBV calculations.

Patient no	rPBV infarct pre	rPBV infarct post	rPBV hypoperfusion pre	rPBV hypoperfusion post	$\Delta$ rPBV infarct	$\Delta$ rPBV hypoperfusion	Follow-up imaging (d = days post procedure)
1	0.644	1.770	0.153	2.638	1.126	2.485	CT (1d)
2	1.229	X	1.227	X	-	-	MRI (1d)
3	0.159	1.353	0.315	1.330	1.194	1.015	CT (1d) + MRI (11d)
4	0.644	X	1.762	X	-	-	CT (1d) + MRI (3d)
5	0.297	X	0.770	X	-	-	CT (1d)
6	0.481	0.968	0.362	2.416	0.487	2.054	CT (1d)
7	0.420	0.283	0.876	0.688	-0.137	-0.188	CT (1d)
8	0.219	X	1.121	X	-	-	CT (1d)
9	0.323	0.989	1.017	0.455	0.666	-0.562	CT (1d)
10	0.212	0.628	0.429	0.813	0.416	0.384	CT (1d)
11	0.541	2.474	0.797	1.230	1.933	0.433	CT (1d)
12	0.179	X	0.884	X	-	-	CT (1d)
13	0.276	0.787	0.573	1.028	0.511	0.455	CT (1d)
14	0.291	1.074	0.263	1.088	0.783	0.825	CT (1d)
15	1.223	1.928	0.282	0.946	0.705	0.664	CT (1d)
16	1.287	X	0.534	X	-	-	CT (1d)
17	1.454	X	0.556	X	-	-	CT (1d)
18	0.486	0.352	0.946	0.982	-0.134	0.036	MRI (1d)
19	0.498	X	1.518	X	-	-	CT (1d)
20	0.607	X	0.663	X	-	-	CT (1d)

Pre indicates pre-recanalization; Post, post-recanalization; rPBV, relative Pooled Blood Volume x: examination not performed.  $\Delta$ rPBV = rPBV pre-rPBVpost; Patients (n = 11) with a pre-and post PBV scan are indicated in green.

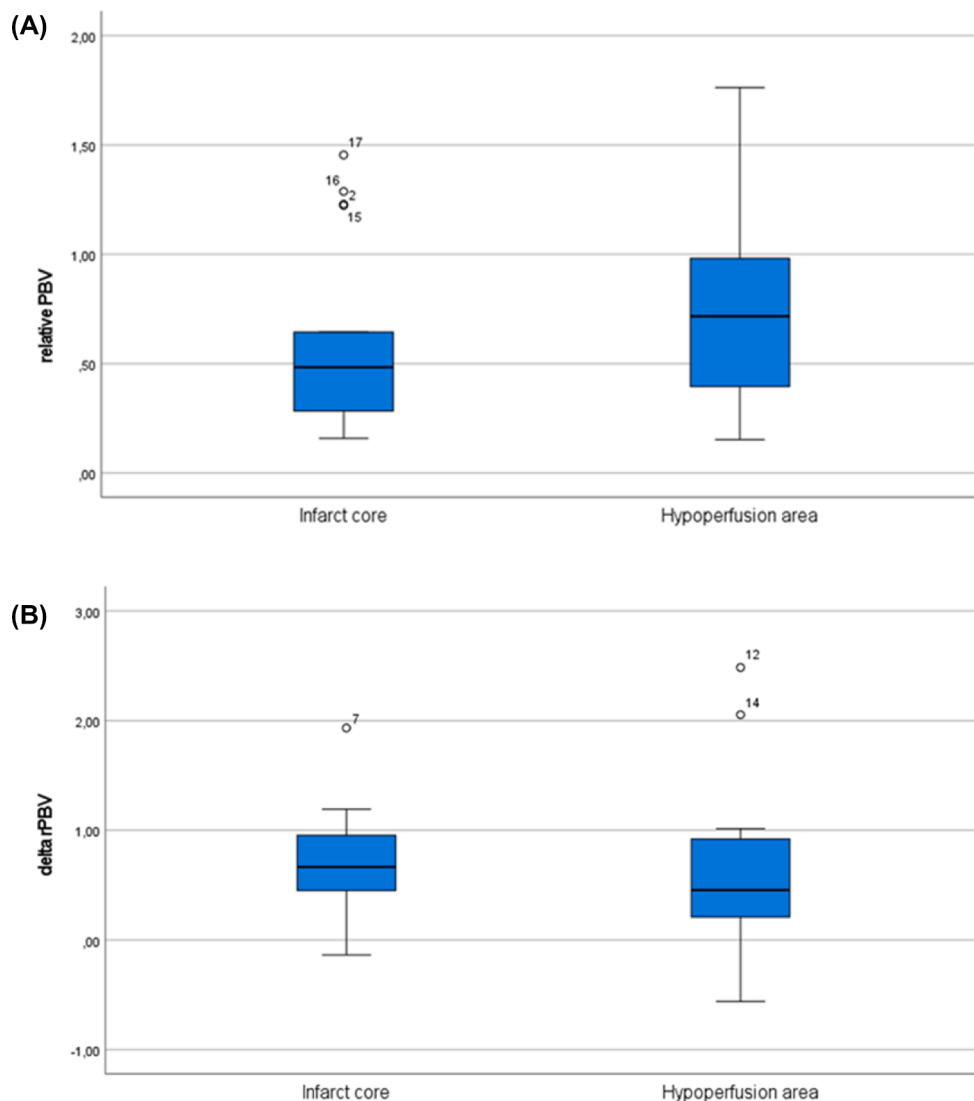


**Fig. 4.** Boxplots of infarct core versus hypoperfusion area of rPBV values in pre-recanalization scans (a) and of pre- and post-recanalization  $\Delta$ rPBV values (b).



score 1). We included the data of these patients as pre-procedural PBV scans, because on follow-up imaging significant mismatch between PBV lesion and final infarct was noted, enabling PBV measurements in hypoperfused brain areas. No procedural complications were noted. Median NIHSS post-procedure (EVT and/or CAS) was 12.5, ranging from 0 to 24. Eight (40 %) patients had a mRS < 3 at 90 days of follow-up and 6 (15 %) patients died during follow-up.

**Table 1** shows patients clinical and radiological measurements.

**Fig. 3** illustrates an example of a patient with PBV scanning before and after EVT.

**Table 2** summarizes the rPBV values and  $\Delta$ rPBV calculations of each patient included in our study. Pre- and post-recanalization rPBV values for infarcted and hypoperfused areas are given.

The mean pre-EVT rPBV values for infarct areas and hypoperfusion areas were respectively 0.57 ( $\pm$ 0.40) and 0.75 ( $\pm$ 0.43). The mean  $\Delta$ rPBV of pre- and post-rPBV values for infarct and hypoperfusion areas were respectively 0.69 ( $\pm$ 0.59) and 0.69 ( $\pm$ 0.90). The average pre and post intervention PBV values for infarct, hypoperfusion and healthy (contralateral hemisphere) are supplied in a supplementary table online.

We did not find a significant difference between the median rPBV value of infarct areas and of hypoperfusion areas ( $p = 0.13$ ). Additionally, there was no significant difference ( $p = 0.62$ ) of  $\Delta$ rPBV between infarct core and hypoperfusion area. In **Fig. 4**, the box plots for rPBV measurements and the  $\Delta$ rPBV values in infarct core and hypoperfusion area are shown.

Due to the non-significant difference between infarct and hypoperfusion rPBV and  $\Delta$ rPBV values, no cut-off threshold could be established.

The calculated effective dose of one PBV acquisition was 2.6 mSv.

## 5. Discussion

In AIS patients, flat panel angiographic PBV mapping can be useful to detect parenchymal perfusion deficit and assess final infarct volume. Unfortunately, in our study, we were not able to differentiate infarcted brain tissue from potentially salvageable tissue based on quantitative PBV measurement.

Final clinical outcome in treatment of AIS patients is strongly related to the time of symptom onset to the time of recanalization [24]. Treatment of AIS patients with LVO requires specialized neurovascular multidisciplinary teams and infrastructures. In many healthcare systems, treatment of AIS patients with a LVO is centralized, implying that patients are moved from primary stroke centers to comprehensive stroke centers. Patient transportation takes time, during which the physiological status of brain areas at risk for infarction may change. Before intended recanalization therapy, repeat cross-sectional imaging with CT or MRI can be useful. Flat panel technology has made it possible to perform a one-stop-shop approach in the angiography suite, using FD-CT techniques to image acute stroke patients. In the neuro-interventional suite, we are able to perform brain parenchyma and brain vessel imaging, rule out hemorrhage, identify early ischemic brain parenchymal changes, and document vascular pathologies [25]. However, the use of FD-CT dynamic perfusion imaging is limited due to restrictions in acquisition of multiple scans in short-time intervals. A way to deal with this problem is by performing perfusion imaging during steady-state contrast filling of the brain, yielding so called PBV maps [10]. The advantages of this technique, compared to dynamic perfusion imaging, are the decreased risk of motion artefacts and reduced total radiation exposure to the patient. Also, PBV imaging can be done on basic angiographic systems.

A feasibility study, comparing FD-CT PBV imaging with conventional CT perfusion (CTP) in 10 AIS patients, demonstrated good correlation between angiographic PBV maps with CBV maps on CTP, suggesting its potential use for differentiating between core infarct and potentially salvageable tissue in AIS patients in the angiography suite [10]. In a study performed by Wagner et al. (2013), comparing AIS patients with

LVO, agreement of areas of distinct PBV decrease with final infarct volume was observed in 15 of the 20 patients studied [26]. They postulated that in the other 5 patients, the larger areas of decreased PBV compared to final infarct area was probably due to inappropriate timing of data acquisition and misery perfusion. Fiorella et al. (2014) confirmed the high sensitivity of PBV maps for detecting CBV deficits defined by prior conventional CT perfusion imaging. They also noticed overestimation of the PBV lesions compared to the CBV lesions [27].

However, the use of CBV as a perfusion parameter for estimating infarct core size in the consideration of recanalization therapy, is subject to debate. Hirai et al. (2021) examined ratios of average CT perfusion CBV values in affected MCA territories to non-lesional contralateral sides in 60 AIS patients and compared those with CBV values obtained from follow-up MRI diffusion imaging [28]. They found that the CBV ratio was a strong predictor of good clinical outcome after successful recanalization, showing good functional outcome in patients with higher CBV values. They propose a threshold CBV ratio of approximately 1, enabling differentiation between patients with good functional and radiological outcomes from those with poor outcomes after recanalization. On the other hand, it is described that raised or normal CBV is not always indicative of salvageable tissue [29].

Only a limited number of papers are published about FD-CT pooled or cerebral blood volume imaging. They demonstrated uncertainty of the nature of PBV maps. In a systematic review, Stille et al. (2019) analyzed the diagnostic accuracy of FD-CT PBV perfusion imaging by comparing PBV values with CBV values derived from conventional CTP in 11 studies, and by comparing FD-CT PBV perfusion accuracy with MRI perfusion CBV values in 5 studies [30]. They concluded that FD-CT provides similar CBV values and reconstructed blood volume maps as CTP in cerebrovascular disease, but they emphasized that additional studies were required. In the aforementioned study by Struffert et al. (2010), a good correlation of angiographic PBV mapping with conventional CTP CBV mapping was found [10]. In another small patient group with AIS in the anterior circulation, the same group of authors (Struffert et al., 2015) confirmed that the perfusion anomalies found on FD-CTP matched with those found on magnetic resonance perfusion (MRP), although the PBV values, corresponded less well with the CBV values acquired with MRI [15].

Kamran et al. (2015) found in a series of 26 patients with delayed cerebral ischemia (DCI) after aneurysmal subarachnoid hemorrhage, that the FD-CT PBV values matched best with a "CBF weighted" CBV parameter on MRP [14]. Nevertheless, by comparing FD-CT PBV data with MRI data in the same patient group, they found that C-arm FD-CT PBV measurements can be used for detection of irreversibly infarcted brain parenchyma [17]. It was possible to define optimal FD-CT PBV (2.49 mL/100 g; area under curve, 0.76; sensitivity, 0.69; specificity, 0.71) and normalized PBV (0.67; area under curve, 0.77; sensitivity, 0.69; specificity, 0.72) thresholds for infarction ( $P$  value < 0.01), based on receiver operating characteristic curve analysis. However, they acknowledged the potential for underestimation of mild ischemia. So far, this is the only (positive) publication about the use of absolute PBV values for infarct determination.

Very few publications exist about the feasibility of PBV technique in AIS patients. Ava et al. (2017) retrospectively evaluated pre-procedural FD-CT PBV scans of 101 patients with AIS referred for EVT [18]. Reconstructed PBV maps and collateral status maps were compared with post-interventional follow-up CT scans. They found that in 75.2 % of the cases the PBV lesion matched with the final infarct and that in the other 24.8 % the final infarct was overestimated on the PBV maps. They concluded that PBV data can be useful for evaluating potential infarct growth and collateral status prior to EVT in case of long time intervals after initial imaging. However, due to the 25 % of final infarct overestimation, they recommended that the FD-CT PBV imaging should not be used as the only basis for patient exclusion. Another study, exploring the prognostic value of pre-procedural FD-CT PBV maps for predicting final infarct volume, was conducted by Mueller et al. (2019) [19].



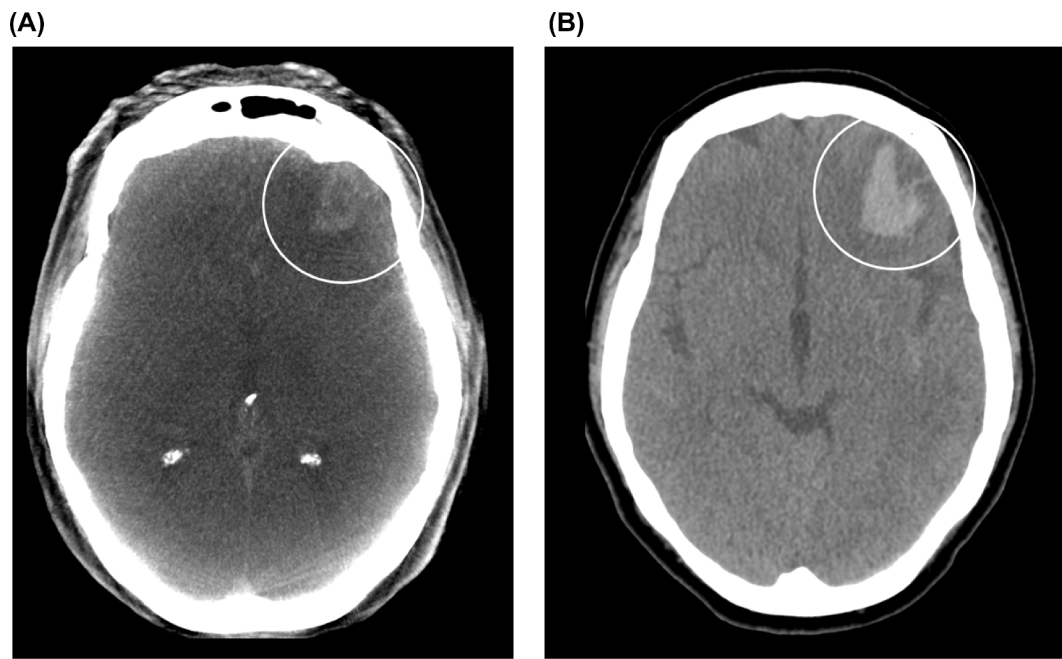


**Fig. 5.** A 52-year-old female patient with a wake-up stroke was referred for EVT. CT angiography and CT perfusion (not shown) was performed in the referring hospital and demonstrated left proximal MCA occlusion with a large perfusion-occlusion mismatch. PBV imaging was performed in the angiography suite before intended EVT procedure. Axial reformatted mask run image (a) demonstrated a hemorrhage (white circle). A follow-up conventional axial non-enhanced CT image (b) 1 day after PBV imaging demonstrated the bleeding site more clearly. Note the clear difference in spatial resolution between the FD-CT PBV mask run MIP reformation and the conventional CT image, making it difficult to detect more subtle signs of infarct on reformatted PBV mask images.

Volumes of PBV deficit found on pre-EVT FD-CT imaging were compared with follow-up CT imaging final stroke volumes in 29 AIS patients with anterior circulation occlusion undergoing EVT. PBV-source images were used for volume calculations. They found that final infarct volume was frequently smaller than the PBV-lesion, especially in the subgroup of successful recanalization. On contrary, patients with futile recanalization showed smaller PBV-lesion volume than the infarct volume at follow-up. In their study, they were not able to detect a significant difference between Hounsfield unit (HU) ratios measured on PBV maps within the ischemic core and the penumbra. Therefore, they finally concluded that FD-CT PBV mapping should not be used in clinical decision making for whether or not performing EVT in LVO stroke. Another, very recently published paper confirms the infarct overestimation by comparing PBV mapping before EVT with follow-up multi-slice CT imaging in about 25 % of the cases [31]. Interestingly, infarct overestimation was observed in conventional CT perfusion CBV mapping as well.

In our study, we were not able to differentiate between infarcted brain tissue or potentially salvageable tissue based on quantitative PBV measurement. There was no statistical significant difference between rPBV values of infarct and non-infarcted areas pre-recanalization therapy nor between  $\Delta$ rPBV values of infarct areas compared to  $\Delta$ rPBV values of non-infarcted hypoperfusion brain areas. Furthermore, we observed a wide range of measured rPBV values and calculated  $\Delta$ rPBV. In patients no. 7 and 18, we detected a decline in PBV value after recanalization therapy. In 4 patients (no. 2, 15, 16 and 17), measured pre-EVT PBV values in infarcted area were higher in the affected side compared to the “normal” contralateral hemisphere. This non-discrepancy of PBV values between core infarct and potential salvageable hypoperfused brain areas might be due to delayed bolus arrival combined with a prolonged vascular transit time in the setting of an upstream LVO, resulting in an underestimation of PBV values in non-infarct areas. This might also partly explain the wide range of the acquired PBV values, reflecting different vascular status of individual patients. A less practical solution might be scanning with increased scanning delay after contrast injection.

A small treatment effect was observed when we looked at the rPBV values of infarcted areas pre-EVT, which significantly increased after EVT. However, an increase in CBV value in the infarct core after recanalization therapy has been previously described [32].

Our study has several limitations. First of all, the study concerned a relative small group of patients in a retrospective analysis. Only 11 patients had optimal pre- and post-PBV scans measurements. Moreover, we used a follow-up multi-slice CT or MRI scan one day post-FD-CT scanning, without conventional CT and/or MRI perfusion imaging as a reference. This might introduce a significant bias, concerning the physiological evolution of brain perfusion in individual stroke patients. Another potential limitation was the performance of PBV imaging by means of arterial contrast injection in the aortic root. It is shown that contrast concentration can differ in the individual carotid arteries significantly after injection by means of a pigtail catheter in the aorta [33]. It is likely that specific anatomical configurations of the aorta and the supra-aortic arteries, together with flow modifying lesions, such as stenosis or occlusions, can have a significant impact on the symmetry of the contrast distribution to the brain. PBV imaging after intravenous contrast injection might yield more symmetrical contrast distribution to the brain. Mainly due to practical reasons, we decided to perform the aortic injection instead of the intravenous contrast injection. An arterial injection fitted better in our clinical routine for the endovascular procedure. In addition, intravenous contrast PBV scanning requires a larger volume of contrast medium injection, which might be a point of concern in patients with preexisting diminished renal function.

We believe that the PBV maps combined with the angiographic MIP “CT angiography” images, derived from the fill run, are only useful for detection of a perfusion deficit due to LVO. In 6 out of the 41 patients (14 %) undergoing FD-CT PBV scanning with only local anesthetics, we experienced major post-processing difficulties due to motion artefacts. The susceptibility of the technique for motion artefacts was also described by Fiorella et al. (2014) [27] and Potreck et al. (2021) [31]. To our experience, the obtained fill run images (FD-CT angiography images) were less susceptible to motion artefacts than the PBV images, enabling sufficiently interpretable images in contrast to the

corresponding PBV maps in 5 out of 6 patients.

The non-contrast FD-CT MIP reformations derived from the mask runs proved to be of very limited value. It was not possible to demonstrate reliable early signs of focal ischemia. However, a significant hemorrhage could be observed, renouncing subsequent recanalization therapy in 2 patients (4 % of scanned initial 49 anterior stroke patients), as demonstrated in Fig. 5.

## 6. Conclusion

Angiographic PBV mapping is technically feasible. A perfusion deficit can be readily distinguished, and, in our experience, the FD-CT PBV images combined with the FD-CT angiography acquisitions derived from the fill run images, can be useful to confirm the presence of LVO in the anterior circulation. The mask images could be used for detection of major hemorrhage, but are of rather poor quality, especially compared with MD CT images. Unfortunately, we were not able to distinguish infarcted tissue from potentially salvageable tissue based on quantitative PBV measurement. In addition, the technique is susceptible to motion artefacts and we experienced difficulties in post-processing, among other things due to beam hardening artifacts. Lastly, the benefit of application of the technique should be weighted carefully against the potential risk of the additional radiation dose administration, using the ALARA (as low as reasonably achievable). Further research is warranted.

## Declaration of Competing Interest

The authors declare that they have no known competing financial interests or personal relationships that could have appeared to influence the work reported in this paper.

## Acknowledgement

The authors would like to thank Patrick Dupont for his support with acquisition.

## References

- [1] Global, regional, and national burden of stroke, 1990-2016: a systematic analysis for the Global Burden of Disease Study 2016, *Lancet Neurol* 18 (5) (2019) 439–458, [https://doi.org/10.1016/S1474-4422\(19\)30034-1](https://doi.org/10.1016/S1474-4422(19)30034-1).
- [2] W.J. Powers, A.A. Rabinstein, T. Ackerson, O.M. Adeoye, N.C. Bambakidis, K. Becker, J. Biller, M. Brown, B.M. Demaerschalk, B. Hoh, E.C. Jauch, C. S. Kidwell, T.M. Leslie-Mazwi, B. Ovbiagele, P.A. Scott, K.N. Sheth, A. M. Southerland, D.V. Summers, D.L. Tirschwell, Guidelines for the Early Management of Patients With Acute Ischemic Stroke: 2019 Update to the 2018 Guidelines for the Early Management of Acute Ischemic Stroke: A Guideline for Healthcare Professionals From the American Heart Association/American Stroke Association, *Stroke* 50 (12) (2019).
- [3] J.L. Saver, Time Is Brain—Quantified, *Stroke* 37 (1) (2006) 263–266.
- [4] M. Rocha, T.G. Jovin, Fast Versus Slow Progressors of Infarct Growth in Large Vessel Occlusion Stroke: Clinical and Research Implications, *Stroke* 48 (9) (2017) 2621–2627.
- [5] C.D. Morgan, M. Stephens, S.L. Zuckerman, M.S. Waitara, P.J. Morone, M. C. Dewan, J. Mocco, Physiologic imaging in acute stroke: Patient selection, *Interv Neuroradiol* 21 (4) (2015) 499–510.
- [6] W.A. Kalender, Y. Kyriakou, Flat-detector computed tomography (FD-CT), *Eur. Radiol.* 17 (11) (2007) 2767–2779.
- [7] L. Zwarzany, W. Poncyjusz, T.H. Burke, Flat detector CT and its applications in the endovascular treatment of wide-necked intracranial aneurysms—A literature review, *Eur. J. Radiol.* 88 (2017) 26–31.
- [8] S.W. Choi, K.W. Jo, Y.W. Kim, S.R. Kim, I.S. Park, H. Kim, Clinical Utility of Angiographic CT with a Flat-detector Angiographic System during Endovascular Procedure, *J Cerebrovasc Endovasc Neurosurg* 18 (3) (2016) 247.
- [9] M. Kamran, S. Nagaraja, J.V. Byrne, C-arm flat detector computed tomography: the technique and its applications in interventional neuro-radiology, *Neuroradiology* 52 (4) (2010) 319–327.
- [10] T. Struffert, Y. Deuerling-Zheng, S. Kloska, T. Engelhorn, C.M. Strother, W. A. Kalender, M. Köhrmann, S. Schwab, A. Doerfler, Flat Detector CT in the Evaluation of Brain Parenchyma, Intracranial Vasculature, and Cerebral Blood Volume: A Pilot Study in Patients with Acute Symptoms of Cerebral Ischemia, *AJNR Am J Neuroradiol* 31 (8) (2010) 1462–1469.
- [11] T. Struffert, Y. Deuerling-Zheng, T. Engelhorn, S. Kloska, P. Göltz, M. Köhrmann, S. Schwab, C.M. Strother, A. Doerfler, Feasibility of Cerebral Blood Volume Mapping by Flat Panel Detector CT in the Angiography Suite: First Experience in Patients with Acute Middle Cerebral Artery Occlusions, *Am. J. Neuroradiol.* 33 (4) (2012) 618–625.
- [12] K. Royalty, M. Manhart, K. Pulfer, Y. Deuerling-Zheng, C. Strother, A. Fieselmann, D. Consigny, C-Arm CT Measurement of Cerebral Blood Volume and Cerebral Blood Flow Using a Novel High-Speed Acquisition and a Single Intravenous Contrast Injection, *AJNR Am J Neuroradiol* 34 (11) (2013) 2131–2138.
- [13] T. Struffert, Y.u. Deuerling-Zheng, S. Kloska, T. Engelhorn, J. Boese, M. Zellerhoff, S. Schwab, A. Doerfler, Cerebral blood volume imaging by flat detector computed tomography in comparison to conventional multislice perfusion CT, *Eur Radiol* 21 (4) (2011) 882–889.
- [14] M. Kamran, J.V. Byrne, C-arm flat detector computed tomography parenchymal blood volume imaging: the nature of parenchymal blood volume parameter and the feasibility of parenchymal blood volume imaging in aneurysmal subarachnoid haemorrhage patients, *Neuroradiology* 57 (9) (2015) 937–949.
- [15] T. Struffert, Y. Deuerling-Zheng, S. Kloska, T. Engelhorn, S. Lang, A. Mennecke, M. Manhart, C.M. Strother, S. Schwab, A. Doerfler, Dynamic Angiography and Perfusion Imaging Using Flat Detector CT in the Angiography Suite: A Pilot Study in Patients with Acute Middle Cerebral Artery Occlusions, *AJNR Am J Neuroradiol* 36 (10) (2015) 1964–1970.
- [16] M. Wintermark, A.E. Flanders, B. Velthuis, R. Meuli, M. van Leeuwen, D. Goldsher, C. Pineda, J. Serena, I.V.D. Schaaf, A. Waaijer, J. Anderson, G. Nesbit, I. Gabriely, V. Quiles, S. Pohlman, M. Quist, P. Schnyder, J. Bogousslavsky, W. P. Dillon, S. Pedraza, Perfusion-CT Assessment of Infarct Core and Penumbra: Receiver Operating Characteristic Curve Analysis in 130 Patients Suspected of Acute Hemispheric Stroke, *Stroke* 37 (4) (2006) 979–985.
- [17] M. Kamran, J.V. Byrne, C-Arm Flat Detector CT Parenchymal Blood Volume Thresholds for Identification of Infarcted Parenchyma in the Neurointerventional Suite, *AJNR Am J Neuroradiol* 36 (9) (2015) 1748–1755.
- [18] L. Ava, J. Berkefeld, A. Lauer, A. Seiler, W. Pfeilschifter, M. Müller-Eschner, S.-J. You, S. Weidauer, U. Pilatus, M. Wagner, Predictive Value of Pooled Cerebral Blood Volume Mapping for Final Infarct Volume in Patients with Major Artery Occlusions. A Retrospective Analysis, *Clin Neuroradiol* 27 (4) (2017) 435–442.
- [19] A. Mueller, M. Wagner, E. Hattingen, A. Seiler, S.-J. You, P. Samp, O.C. Singer, Flat Panel Computed Tomography Pooled Blood Volume and Infarct Prediction in Endovascular Stroke Treatment, *Stroke* 50 (11) (2019) 3274–3276.
- [20] T. Brott, H.P. Adams, C.P. Olinger, J.R. Marler, W.G. Barsan, J. Biller, J. Spilker, R. Holleran, R. Eberle, V. Hertzberg, Measurements of acute cerebral infarction: a clinical examination scale. *Stroke* 20 (7) (1989) 864–870.
- [21] J.C. van Swieten, P.J. Koudstaal, M.C. Visser, H.J. Schouten, J. van Gijn, Interobserver agreement for the assessment of handicap in stroke patients. *Stroke* 19 (5) (1988) 604–607.
- [22] R.T. Higashida, A.J. Furlan, Trial Design and Reporting Standards for Intra-Arterial Cerebral Thrombolysis for Acute Ischemic Stroke, *Stroke* 34 (8) (2003).
- [23] L.-L. Wen, X. Zhang, Q.-R. Zhang, Q.i. Wu, S.-J. Chen, J.-L. Deng, K. Huang, H.-D. Wang, Flat-detector computed tomography PBV map in the evaluation of presurgical embolization for hypervascular brain tumors, *J NeuroIntervent Surg* 9 (11) (2017) 1139–1144.
- [24] M. Goyal, A.P. Jadhav, A. Bonafe, H. Diener, V. Mendes Pereira, E. Levy, B. Baxter, T. Jovin, R. Jahan, B.K. Menon, J.L. Saver, Analysis of Workflow and Time to Treatment and the Effects on Outcome in Endovascular Treatment of Acute Ischemic Stroke: Results from the SWIFT PRIME Randomized Controlled Trial, *Radiology* 279 (3) (2016) 888–897.
- [25] A. Doerfler, P. Göltz, T. Engelhorn, S. Kloska, T. Struffert, Flat-Panel Computed Tomography (DYNA-CT) in Neuroradiology. From High-Resolution Imaging of Implants to One-Stop-Shopping for Acute Stroke, *Clin Neuroradiol* 25 (S2) (2015) 291–297.
- [26] M. Wagner, Y. Kyriakou, R. du Mesnil de Rochemont, O.C. Singer, J. Berkefeld, Does Preinterventional Flat-Panel Computer Tomography Pooled Blood Volume Mapping Predict Final Infarct Volume After Mechanical Thrombectomy in Acute Cerebral Artery Occlusion? *Cardiovasc Intervent Radiol* 36 (4) (2013) 1132–1138.
- [27] D. Fiorella, A. Turk, I. Chaudry, R. Turner, J. Dunkin, C. Roque, M. Sarmiento, Y. u. Deuerling-Zheng, C.M. Denice, M. Baumeister, A.T. Parker, H.H. Woo, A prospective, multicenter pilot study investigating the utility of flat detector derived parenchymal blood volume maps to estimate cerebral blood volume in stroke patients, *J NeuroIntervent Surg* 6 (6) (2014) 451–456.
- [28] S. Hirai, Y. Tanaka, H. Sato, K. Kato, Y. Kim, T. Yamamura, K. Sumita, T. Arai, Quantitative collateral assessment evaluated by cerebral blood volume measured by CT perfusion in patients with acute ischemic stroke, *J. Stroke Cerebrovasc. Dis.* 30 (7) (2021) 105797.
- [29] C.D. d’Esterre, G. Roversi, M. Padroni, A. Bernardoni, C. Tamborino, A. De Vito, C. Azzini, O. Marcello, A. Saletti, S. Ceruti, T.Y. Lee, E. Fainardi, CT perfusion cerebral blood volume does not always predict infarct core in acute ischemic stroke, *Neuro Sci* 36 (10) (2015) 1777–1783.
- [30] E.L. Stille, I. Viozzi, M. ter Laan, F.J.A. Meijer, J.J. Futterer, M.M. Rovers, Diagnostic accuracy of flat-panel computed tomography in assessing cerebral perfusion in comparison with perfusion computed tomography and perfusion magnetic resonance: a systematic review, *Neuroradiology* 61 (12) (2019) 1457–1468.
- [31] A. Potreck, A. Falbesaner, F. Seker, C.S. Weyland, S. Mundiyanapurath, S. Heiland, M. Bendszus, J.A.R. Pfaff, Accuracy and reliability of PBV ASPECTS, CBV ASPECTS

- and NCCT ASPECTS in acute ischaemic stroke: a matched-pair analysis, *Neuroradiol J* 34 (6) (2021) 585–592.
- [32] A.R. delpolyi, O. Wu, E.A. Macklin, P.W. Schaefer, L.H. Schwamm, R. Gilberto Gonzalez, W.A. Copen, Reliability of cerebral blood volume maps as a substitute for diffusion-weighted imaging in acute ischemic stroke, *J. Magn. Reson. Imaging* 36 (5) (2012) 1083–1087.
- [33] Q. Zhang, R. Xu, Q. Sun, H. Zhang, J. Mao, T. Shan, W. Pan, Y. Deuring-Zheng, M. Kowarschik, J. Beilner, Exploring the Value of Using Color-Coded Quantitative DSA Evaluation on Bilateral Common Carotid Arteries in Predicting the Reliability of Intra-Ascending Aorta Flat Detector CT–CBV Maps, *AJNR Am J Neuroradiol* 36 (5) (2015) 960–966.